Nanofluidic tools for bioanalysis : the large advantages of the nano-scale

Janssen, K.G.H.

CHAPTER 3

Limits of miniaturization: Assessing ITP performance in sub-micron and nanochannels[a]

3.1 Abstract

The feasibility of isotachophoresis in channels of sub micrometer and nanometer dimension is investigated. A sample injection volume of 0.4 pL is focused and separated in a 330 nm deep channel. The sample consists of a biomatrix containing the fluorescently labeled amino acids glutamate and phenylalanine, 20 attomoles each. In a 50 nm deep channel, isotachophoretic focusing is successfully demonstrated. Separation of the two amino acids in the 50 nm deep channel however, could not be performed as the maximum applicable voltage was insufficient. This limit is imposed by bubble formation that we contribute to cavitation as a result of the mismatch in electro-osmotic flow, so called electrocavitation. This represents an unexpected limit on miniaturization of ITP. Nonetheless, we report the smallest isotachophoretic separation and focusing experiment to-date, both in terms of controlled sample injection volume and channel height.

[a]Published as: Kjeld G. H. Janssen, Jiajie Li, Hanh T. Hoang, Paul Vulto, Richard J. B. H. N. van den Berg, Herman S. Overkleeft, Jan C. T. Eijkel, Niels R. Tas, Heiko J. van der Linden and Thomas Hankemeier, *Lab On a Chip*, **12**, 2888, (2012).

3.2 Introduction

The last three decades, major efforts have been invested in the miniaturization of elecktrokinetic separation techniques, such as zone electrophoresis, iso-electric focusing and isotachophoresis[32–35]. With the advent of nanochannel fabrication technologies[43] emphasis has shifted towards the nanofluidic domain. So far, liquid chromatography[44,45] and zone electrophoresis[46,47] have been successfully demonstrated in a nanofluidic environment.

Isotachophoresis (ITP) particularly benefits from downscaling as the resolution in equilibrium increases with decreasing channel cross-section, for a given amount of analyte. This inherent benefit originates from the fact that ITP is a concentration driven focusing technique. In equilibrium, the achieved concentration depends on the absolute amount of analyte, independent of initial concentration or sample volume. When available in sufficient amounts, a maximum concentration is reached and analytes are separated in neighboring zones, so called plateau mode ITP. The plateau concentration depends amongst others on the concentration of the leading electrolyte (LE) and the mobility of the analyte[53–56]. In ITP the resolving power can be expressed as a signal-to-noise ratio (SNR) given by the length of the analyte plateau zone normalized by the characteristic length of diffused zone boundaries[58,60]. Upon downscaling the cross-section of an ITP channel, a correspondingly lower absolute amount of analyte is required to achieve the same ITP equilibrium concentration and separation. Therefore, with the absolute amount conserved, downscaling the cross section by a certain factor, the same amount of compound will occupy a correspondingly longer section of channel, thereby improving resolution and signal to noise ratio for ITP in equilibrium by the same factor. In case of a detector based on absolute amount per length of channel a trade-off needs to be considered between better separation of compounds vs a lower signal per channel length and longer analysis times. If not enough absolute amount of analyte is present, the plateau concentration is not reached, and analytes focus as peaks (so-called peak mode ITP) that may overlap partially or even completely[58]. Sufficient downscaling will then allow these compounds to be focused at a higher concentration in equilibrium or even to form plateaus and be separated.

An important proof-of-principle of ITP downscaling has been delivered by Walker et al.[61], who were the first to demonstrate ITP in a microfluidic device. Since then, many applications of ITP in the microfluidic chip-platform have been reported, as extensively reviewed elsewhere[33,62,63]. Jung et al. showed that concentration factors up to a million times can be achieved due to downscaling to microfluidic dimensions[57]. A systematic theoretical and experimental study demonstrating the advantages of cross-section miniaturization on ITP was performed in microchannels[60]. Electroosmotic flow (EOF) profiles in nanochannels are parabolic[38]. Parabolic flow increases dispersion in microchannels, and for ITP specifically, it increases dispersion from EOF mismatch due to ion density gradients[102,103]. In nanochannels, however, the contribution to dispersion from

parabolic flow profiles becomes advantageously insignificant, as reflected in the low Peclet number associated with this scale[46].

Notwithstanding the inherent gain of miniaturization on isotachophoretic performance the micrometer threshold has, to our knowledge, not been crossed in peer-reviewed publications. This stagnation may be explained by the many complications that occur when dealing with sub-micrometer channels, as this scale is dominated by nanoeffects[37–41]. The very large surface-to-volume ratio in a nanochannel increases the influence of the electrochemical double layer (EDL)[48]. When channel dimensions approach that of the EDL, electrophoretic separations of ionic analytes are affected, as separation also occurs based on valence, rather than on mobility only[46,47,104]. The extremely large surface to volume ratio favors chromatographic effects as exploited in nano-chromatography[44]. This influences the apparent electrophoretic mobility and diffusion rates of ions[105] and ampholytes[106]. Furthermore, the surface of siliconoxide nanochannels (e.g. glass) dominates the pH of the solution, as demonstrated by a lowering of the solution pH by 6 units despite the presence of a 1 mol/L TRIS buffer[107].

Since many boundary conditions of isotachophoresis are affected by downscaling to sub-micrometer dimensions, a reconsideration of experimental conditions is required. An important observation is that positive-mode ITP in a negatively charged nanochannel (i.e. glass) can be expected to be seriously hampered due to analyte-wall interactions. Conventionally, ITP ion density gradients are preferably chosen as large as possible to maximize the focusing efficiency, e.g. 1 mol/L for the LE versus 5 mmol/L for the TE[57]. In nanochannels this ratio needs to be as small as possible to circumvent wall-induced titration effects[107]. On the other hand, the fact that ITP is a focusing technique renders it more resilient against nanofluidic dispersion effects than any other electrokinetic separation technique.

In this work we demonstrate the feasibility of ITP in sub micrometer and nanochannels. We present an experimental framework that allows direct translation of conventional capillary separation protocols to sub-micrometer platforms. We show that this approach enables focusing and separation of attomole quantities of amino acids, from a controlled volume of injected sample. Finally, the limits on ITP miniaturization were explored in nanochannels, yielding the discovery of a fundamental boundary on ITP downscaling imposed by the nanoscale dimension.

3.3 Experimental

3.3.1 Chip design & fabrication

Chip devices were made from borofloat glass wafers (SCHOTT AG, Mainz, Germany). In the bottom-side wafer, nanochannels and rulers were made by HF etching[43]. The nano and sub-micron channels were 50 nm deep and 10 µm wide and 330 nm deep and 3 µm wide, respectively. Chip devices consisted exclusively

of one channel depth. The depths of the channels were measured with a Dektak 8 mechanical surface profiler (Veeco Instruments Inc. Plainview, USA). Access holes were powderblasted in the bottom-side and top-side wafers. This allows fluidic and electric interfacing from opposite sides. Wafers were placed for several hours in an ultrasonic bath with deionized water. Then the wafers were transferred into 100% HNO_3 and left for 15 min, followed by thorough rinsing with water and finally spin-drying. The wafers were aligned, contacted and fusion bonded at 600 °C for 4 hours. Immediately prior to experiments, the wafers were pre-conditioned at 400 °C for 2 hours in air, improving reproducibility between measurements.

Figure 3.1 shows the layout of the chips. The configuration of channels and access holes incorporates T-junctions (Figure 3.1) that allow a sample volume to be interposed between a leading electrolyte (LE) and a trailing electrolyte (TE) and selection of different injection volumes. A 400 µm injection length corresponds to a volume of 0.2 pL and 0.4 pL, for the nano and sub-microchannel respectively.

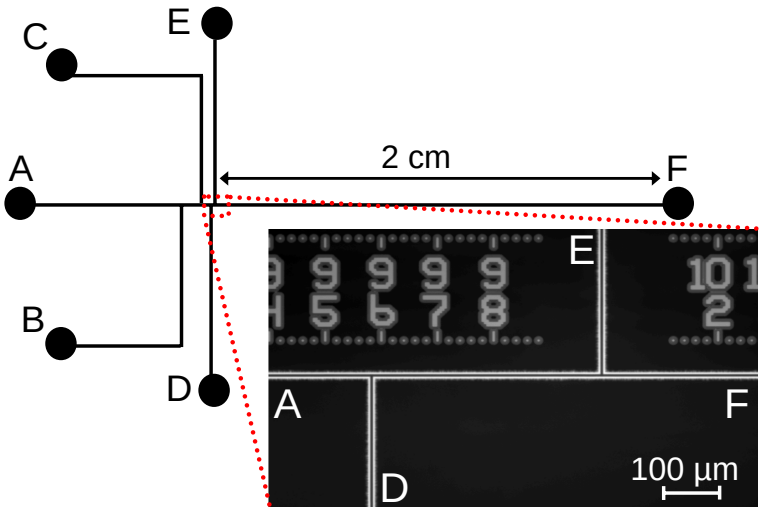

Figure 3.1 Schematic layout of the nanofluidic-ITP chip. A-F designate the access holes, approximately 1 mm in diameter, for placement of electrodes and fluidic access. The insert shows a brightfield image of the injection area where channels D and E intersect with the separation channel, 400 µm apart. The ruler etched along the separation channel, has 20 µm spacing between minor divisions, with the numbers at the major divisions indicating hundreds of microns.

3.3.2 Setup

For on-chip nano-ITP experiments, brightfield and fluorescence imaging was performed with a Olympus BX51WI microscope, equipped with a longpass filter cube (488 nm excitation, 518 nm emission) and a 10x magnification lens, numerical

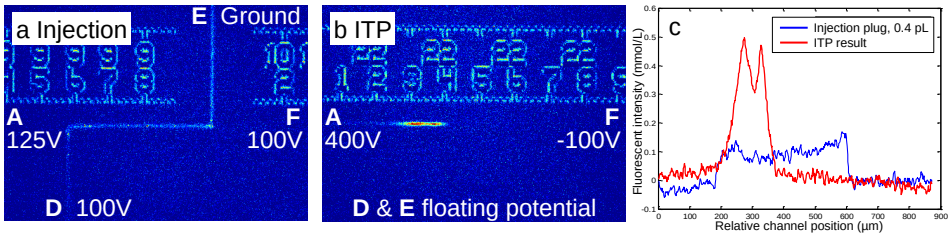

Figure 3.2 On-chip ITP results in 330 nm deep channels for 0.4 pL of yeast matrix spiked with Glu-FITC and Phe-FITC. The letters A, D, E and F refer to the sample reservoirs designated in Figure 3.1, with corresponding voltages applied. a) An injection plug was successfully inserted in between of a leading (left side) and trailing electrolyte (right side). b) Isotachophoretic focusing and separation of Glu-FITC and Phe-FITC into distinguishable peaks. c) Overlay of the injection plug and the separation profile scaled to concentration.

aperture 0.25 (Olympus Corporation, Tokyo, Japan). Electric potentials were applied and monitored using a HSV488 6000D power supply (LabSmith inc., Livermore, USA), controlled through the included Sequence software. Images and movies during experiments were acquired with a Hamamatsu Orca-ER CCD camera and included HoKaWa software (HAMAMATSU Photonics K.K., Japan). Digital (pre) processing and analysis of the data, images and movies was performed using Matlab (MathWorks Inc., Natick, USA).

A custom-built chip interface provided a standardized electrode arrangement from below and reservoirs from the top, aligned with the chip's access holes. The reservoirs were sealed to prevent evaporation and minimize interaction with CO_2 as this influences ITP experiments[108,109].

The movie frames from fluorescence experiments shown in this paper were false coloured for intensity. Intensity profiles from such images were extracted along the separation channel A-F (Figure 3.1), creating an intensity graph.

3.3.3 Isotachophoresis procedure

The amino acids glutamate and phenylalanine labeled with fluorescein isothiocyanate (FITC) were selected as analytes (see Appendix 3.7.1 for labeling and purification procedure). The electrophoretic mobilities of those analytes were determined with capillary zone electrophoresis (see Appendix 3.7.2). Test analytes were spiked to a biomatrix of metabolites extracted from hydrolysate of delipided yeast biomass of *P. pastoris* (see Appendix 3.7.3). The ITP protocol was developed in conventional capillary format (see Appendix 3.7.4). The leading electrolyte (LE) was 10 mmol/L of NaCl and the trailing electrolyte (TE) 5 mmol/L of HEPES. Both electrolytes were adjusted to a pH of 9.50 with sodium hydroxide, verified with a Hanna HI 4521 pH meter (HANNA instruments Inc. Woonsocket,

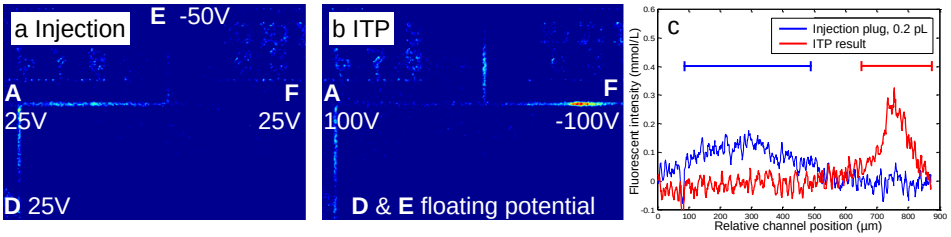

Figure 3.3 On-chip ITP results in 50 nm deep channels for 0.2 pL of yeast matrix spiked with Glu-FITC and Phe-FITC. The letters A, D, E and F refer to the sample reservoirs designated in Figure 1, with corresponding voltages applied. a) An injection plug is successfully inserted in between of a leading (left side) and trailing electrolyte (right side). b) Isotachophoretic focusing of Glu-FITC and Phe-FITC. c) Overlay of the injection plug and the focused zone scaled to concentration. The blue and red bar designate the injection plug length and focused ITP zone length, respectively.

USA) and stored under argon until used [b]. The sample consisted of 70:20:5:5 (v:v:v:v) of TE, yeast cell extract in DMSO, and the fluorescently labeled amino acids phenylalanine and glutamate solutions (1 mmol/L solution in DMSO), respectively. The final concentration of analytes in the sample was 50 µmol/L.

Trailing electrolyte was placed in reservoir F (Figure 3.1), whereupon the channels were filled by capillary action[95], typically within a few minutes. When the chip was completely filled, TE was also applied in well E, LE in well A and the sample solution in well D, wells B and C were left empty. The electrolyte arrangement characteristic for conventional ITP, with the sample volume interposed between the leading and trailing electrolyte was achieved by means of EOF and the double T-structure (Figure 3.1). The appropriate voltage settings on the reservoirs for sample plug formation and those for ITP were obtained empirically and incorporated in an automated protocol of the Labsmith Sequence software. For details and development of the injection procedure see Appendix 3.7.5.

3.4 Results & Discussion

3.4.1 Isotachophoresis in sub-micrometer channels

Figure 3.2 demonstrates an injection, isotachophoretic focusing and separation of 0.4 pL of amino-acid spiked yeast extract in a sub-micron channel (330 nm deep). In order to enable quantitative interpretation of the results we adapted the classical T-injection strategy from electrophoresis chips to our nano-ITP platform. The injection approach used (Appendix 3.7.5) enabled us to achieve a precisely defined injection volume of 0.4 pL as can be seen in Figure 3.2a. This injection

[b]Note that HEPES is not in its buffering domain and therefore cannot be considered a buffer, nor is NaCl a buffer. Although buffers should normally be used, this was done to evaluate potential titration from the nanochannel, see introduction

volume was 300,000 times smaller than that used in the experiments in capillary (0.12 µL) and constitutes absolute quantities of 20 attomole of each labeled amino acid. Figure 3.2b shows the downstream focusing and separation of the fluorescently labeled Glu-FITC and Phe-FITC. The fluorescent intensities in the CCD images in Figure 3.2a,b, were extracted and scaled to concentration (see overlay Figure 3.2c). The area under the curve of the sample plug and focused peaks were compared. It was found that the peak area of the ITP result was in roughly qualitative agreement with that of the plug, indicating that the complete injection plug has been focused and no significant losses have occurred.

Figure 3.2 clearly shows that separation was achieved. The profile appears to correspond to peak mode ITP equilibrium. In order to verify this, we injected a larger sample volume of 3.2 pL (Appendix 3.8.1), which showed higher peaks instead of broader plateaus. Separation in peak mode is typically poor. Nevertheless we observe clear distinguishable peaks. The explanation for this is that the biomatrix provides spacer compounds which focus in between the two fluorescent analytes. This was verified by injecting a larger volume (Appendix Figure 3.9) as well as by conventional capillary ITP (Appendix Figure 3.6).

The above result indicates that translation of conventional ITP protocols to sub-micrometer channels is feasible. As a side result, to our knowledge, this work demonstrates for the first time the implementation of a cross T injection for isotachophoresis. Larger injection volumes can easily be facilitated on a chip. An elegant way to incorporate larger sample volumes for ITP is by means of a large cross section followed by a smaller one, combining the higher sample volume compatibility of the larger one with the improved resolving power of the smaller one. This approach was already introduced by Everaerts et al.[53] and its theory and benefits were recently studied extensively[60]. This geometry can be applied for instance to offset dilution from pretreatment, diffusion or world-to-chip interfacing[110] in order to conserve the amount of analyte and still make use of the improved focusing and separation in a nanochannel. A nanochannel as demonstrated here could well be used as the small cross-section part of such a geometry.

The miniaturization of analysis techniques for sub-pL sample volumes is of great importance in biological and clinical applications. Firstly, extraction of such small volumes is expected to reduce invasiveness; lower sample consumption allows increased temporal resolution of processes measurements and/or multiple parallel studies on conventional sample volumes. Particularly the analysis of single cells is an important example, promising unprecedented insights in cell biology[111,112]. Whole cell analysis has motivated the miniaturization of analysis platforms[113,114], for which electrophoretic techniques were successfully applied[115–119]. The results in this paper, for absolute quantities of 20 attomole of each analyte in a biomatrix can be directly translated to whole cell ITP analysis of a 25 µm cell, for analytes at a concentration of $\approx$ 2.5 µmol/L. However, to study a cell's intracellular time-resolved metabolism, in e.g., cellular division, apoptosis, differentiation, or its response to drugs and stress, time resolved analysis

Figure 3.4 Brightfield image of bubbles in a 50 nanometer deep channel, visible as brighter regions, formed during ITP, during ITP at 500 V. in the 50 nm deep channel.

of sub-cellular aliquots is required. Thus the bioanalyis of sub picoliter sample volumes and resolving the correspondingly low amounts of analytes is an important challenge. The 0.4 pL of injection volume demonstrated here corresponds directly to a sample volume of 5% from a 25 micron cell. Analysis of such minute quantities and volumes as shown here represents the achievement of an important downscaling milestone and indicates that nano-ITP has great potential as the separation component in a single cell or subcellular aliquot analysis platform.

3.4.2 Isotachophoresis in nanochannels

To investigate the limit of downscaling, we performed ITP in a fluidic chip consisting exclusively of nanochannels (50 nm deep) (see Figure 3.3 and Appendix 3.8.3). Concentrations and composition of sample were identical to those used in Figure 3.2. As can be seen in Figure 3.3a and b, sample injection could be performed followed by isotachophoretic focusing. Unfortunately we were not able to inject the complete sample volume. Based on the overlay in Figure 3.3c, we estimate an injection loss of 42%. A separation into separate peaks could not be observed for the voltages used here. Application of higher voltages (500 V) in this channel depth lead to bubble formation in the channel (see Figure 3.4).

Given the extremely high surface to volume ratio and corresponding efficient heat transfer plus the fact that we did not observe bubble formation at this voltage in larger channels, allows the conclusion that this phenomenon is unlikely to result solely from Joule heating effects. The phenomenon of bubble formation is likely explained by cavitation, induced by extreme pressure gradients originating from EOF mismatch between electrolyte zones in nanochannels. As such it may not only affect ITP in nanochannels, but other techniques using concentration gradients as well. First findings on electrocavitation have been reported[120], and a full paper is in preparation.

Table 3.1 compares conditions and results achieved for the sub-micron channels and the nanochannels. For 200 V, isotachophoretic focusing, but not sepa-

ration, was demonstrated in sub-micron channels (Appendix Figure 3.10) as well as in nanochannels (Figure 3.3). In sub-micrometer channels both focusing and separation could be achieved for potentials of 500 V. In the nanochannels such higher voltages lead to the formation of bubbles, and separation could not be demonstrated. The 500 V applied for 330 nm deep channels also represents an upper limit, above which bubble formation occurred. This corresponds to 75% of the electric field used in capillary ITP (Appendix 3.7.4). Nonetheless, in contrast to the nanochannels, the applicable potential was still sufficient for separation. These results indicate that a limit of downscaling for ITP using standard protocols is reached.

Table 3.1 Summary of ITP settings for sub-micron and nanochannels and their corresponding performance.

Channel depth	Injected vol.	Potential	Focusing	Separation
330 nm	0.4 pL	200 V	yes	no
330 nm	0.4 pL	500 V	yes	yes
50 nm	0.2 pL	200 V	yes	no
50 nm	0.2 pL	500 V	bubble formation	bubble formation

3.5 Conclusions & Perspectives

In this paper we have investigated the scalability of conventional ITP into the nanofluidic domain. We have shown isotachophoretic focusing and separation in sub-micrometer channels, which, to our knowledge, represents the smallest demonstration of ITP focusing and separation to date, both in terms channel dimension and injection volume. Separation was performed in the presence of a biomatrix, demonstrating real-sample compatibility. Also, the concept of ITP spacers was shown to be conserved. A controlled quantitative injection scheme based on a double-T geometry was for the first time implemented for ITP, demonstrating that quantitative assessment of analyte composition is feasible. Subsequently, we demonstrated isotachophoretic focusing in 50 nm deep channels. Separation, however, could not be achieved as the applicable voltage was restricted by bubble formation in the channel. Despite successfully circumventing known nanodimension complications, we encountered an unexpected limit of ITP efficiency upon downscaling. Future research will focus on a more precise assessment of the restrictions on ITP miniaturization, including the origins of the bubble formation. Last but not least, we have shown the applicability of ITP to subcellular volumes containing attomoles of analyte and will continue our efforts to enable a subcellular analysis platform by means of low volume ITP. Despite the miniaturization limit reported here, ITP remains best positioned for effective downscaling and bioanalysis of ultra low compound quantities.

3.6 Acknowledgements

We gratefully acknowledge Raphaël C.T. Zwier from the Department of Fine Mechanics (Leiden University, The Netherlands) for his skilled and extensive work on the interfacing. Professor Rainer Bisschof (Groningen University, The Netherlands) is thanked for giving us the PACE system. Dr. Tatjana Egorova (Protein Labeling Innovation, Leiden, The Netherlands) is acknowledged for supplying the yeast sample. This project was financed by NanoNed, an initiative of the Dutch Science and Technology Foundation (STW), the Netherlands Metabolomics Centre, the Netherlands Genomics Initiative and the Netherlands Organization for Scientific Research (NWO).

3.7 Appendix, Methods

3.7.1 Fluorophore labeling of amino acids

All chemicals were acquired from Sigma-Aldrich Co. (Zwijndrecht, The Netherlands), unless noted otherwise. Labeling of glutamate, phenylalanine, and leucine with fluorescein isothiocyanate (FITC) was performed as follows. To 0.5 mmol of amino acid an aqueous solution of potassium hydroxide, 1 g/ml, was added in a ratio of 1:1 (weight:volume), followed by addition of 1 ml of ethanol. Under vigorous stirring, on ice, a suspension of FITC, 1 mol/L in ethanol was added to the amino acid 1:1 (mol:mol) together with 1 ml 0.5 mol/L potassium hydroxide and 0.5 mL ethanol. This mixture was left on ice to react for 2 h in the dark under continued stirring. Purification of the reaction product was performed using a Gilson preparative HPLC system (Gilson, Inc., Middleton, USA) equipped with a Phenomex Gemini C18 column, 15x21 mm, 5 micron (Phenomenex, Torrance, USA) using an acetonitrile/water (10 mmol/L ammonium acetate, pH = 8) gradient. Purity of compounds was established with liquid chromatograpy ultraviolet mass spectrometry (LC-UV-MS) and CZE-LIF and found to be $>$99%. After freeze-drying, each purified FITC-amino was dissolved in dimethyl sulfoxide (DMSO), 1 mmol/L, and stored at -80 $^{\circ}$C awaiting experiments.

FITC, having a pKa of 6.7[92], fluoresces strongly when negatively charged at valence -2. FITC labeled biosamples are of general interest. FITC-labeled amino acids have been studied with CZE[24,121,122] chip ZE[32,123] and ITP in capillary[124–126] and microchannels[127] as well as other techniques[128]. As unpurified reaction product is used almost exclusively in these publications, the two most abundant fluorescent by-products of this labeling are considered to be of interest and were purified and identified with LC-UV-MS (Data not shown). One reaction by-product consisted of FITC where its isothiocyanate group (-N=C=S) was degraded to an amine, which in turn reacted with FITC thus forming a fluorescent dimer (MW 737). As degraded FITC was low abundant in the reaction mixture this implied that the degradation was slower than the reaction with another FITC molecule. This dimer has an almost 4 times lower fluorescent intensity (at 488 nm excitation, 514 nm emission) compared to FITC, due in part to a shifted fluorescence wavelength optimum. The other abundant by-product (MW 436) was FITC that had reacted with ethanol (-N=C-S-O-C_2H_5). FITC is commonly dissolved in ethanol, but our data suggests this should be avoided.

3.7.2 Capillary electrophoresis

A PACE 5000 capillary electrophoresis apparatus equipped with laser-induced-fluorescence detection, operating at 488 nm excitation and 518 nm emission (Beckman Instruments, USA) was used for CZE. CZE was applied to determine the mobilities of the FITC-amino acids as well as establishing their purity for the purpose of fluorescence measurements. The temperature during all experiments

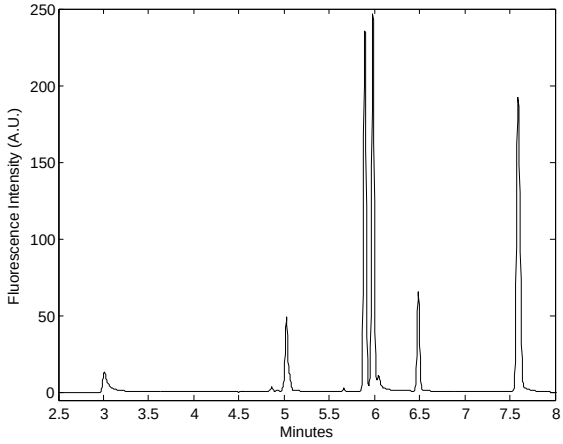

Figure 3.5 Typical CZE electropherogram of labeled amino acids and FITC by-products. From left to right first at 3 minutes the EOF marker bodipy is seen, then FITC-ethanol, leucine-FITC, phenylalanine-FITC , fluorescein amine-FITC and glutamate-FITC, all except FITC-Ethanol at 10 µmol/L.

was maintained at 25 °C by the instrument thermostat. The fused silica capillary (Inacom Instruments, Overberg, The Netherlands) used for CZE had a 50 µm inner diameter and a total length of 56.9 cm measuring 50.3 cm from inlet to detector. Runs were performed at 20 kV, giving a typical current of 14.4 ± 0.1 µA during runs. The background electrolyte was a 10 mmol/L solution of disodium tetraborate ($Na_2B_4O_7$). It was adjusted to pH = 9.50 with sodium hydroxide solution (to ensure maximum fluorescence intensity of fluorescein, as this is pH dependent pKa = 6.7[92]), verified with a Hanna HI 4521 pH meter (milli-pH unit resolution, HANNA instruments Inc. Woonsocket, USA). As a marker for the electro-osmotic flow (EOF) the uncharged fluorophore 4,4-difluoro-4-bora-3a,4a-diaza-s-indacene (bodipy), was added.

CZE of the labeled amino acids and the two reaction by-products was performed establishing their purity for fluorescence measurements (Appendix Figure 3.5). Their calculated electrophoretic mobilities are given in Table 3.2. Based on their mobility phenylalanine-FITC and glutamate-FITC were selected for the ITP protocol, as their difference increased the potential of spacing by compounds in the yeast biomatrix. As ITP electrolytes, chloride was chosen as leading ion, 4-(2-hydroxyethyl)-1-piperazine-ethanesulfonic acid (HEPES) as trailing ion and sodium as the common counterion (See Table 3.2).

3.7.3 Yeast pretreatment for metabolite extraction

To hydrolysate of delipided yeast biomass of *P. pastoris* (YPp(N)-HyBm1, Protein Labeling Innovation PLI, Leiden, The Netherlands) cold (-20 °C) 80:20 methanol:

Table 3.2 Electrophoretic mobilities (μ) and valences at pH 9.5 of the FITC labeled amino acids, FITC by-products and the ions in the ITP electrolytes.

Ion	valence	μ $(10^{-9}\mathrm{m^2V^{-1}s^{-1}})$
HEPES[56],(trailing ion)	-1	-21.8
FITC-ethanol	-2	-31.5
Leucine-FITC	-3	-38.4
Phenylalanine-FITC	-3	-39.0
Fluorescein amine-FITC	-4	-42.0
Glutamate-FITC	-4	-47.3
Chloride[55], (leading ion)	-1	-79.1
Sodium[55], (counter ion)	+1	51.9

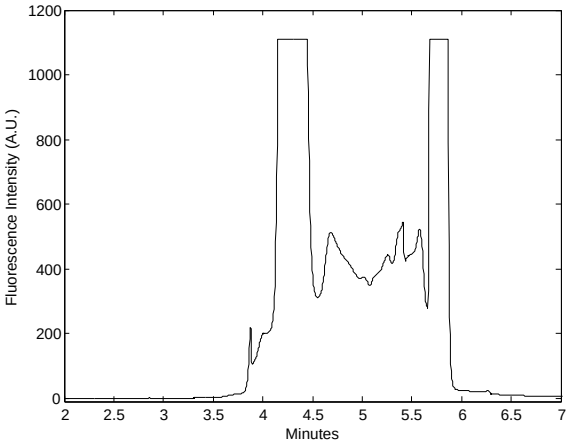

Figure 3.6 Capillary-ITP for a 0.12 μL sample of yeast biomatrix and 5 glutamate-FITC and phenylalanine-FITC both 50 μmol/L. The measurement using LIF shows from left to right, Phe-FITC and Glu-FITC, spaced by the yeast biomatrix, with TE to the left and LE to the right of the sample.

water was added. After placement for 30 minutes in an ultrasonic bath, this mixture was centrifuged and the supernatant collected. This extraction procedure was repeated and the combined supernatants were freeze-dried, after removal of methanol. These extracted compounds were redissolved in dimethyl sulfoxide (DMSO) to 10 mg/mL (relative to the original weight of the hydrolysate prior to pretreatment) and stored at -80 °C awaiting experiments.

3.7.4 Isotachophoresis protocol development in capillary

A PACE 5000 capillary electrophoresis apparatus equipped with laser-induced-fluorescence detection, operating at 488 nm excitation and 518 nm emission (Beckman Instruments, USA) was used for ITP experiments. The temperature during all experiments was maintained at 25 °C by the instrument thermostat.

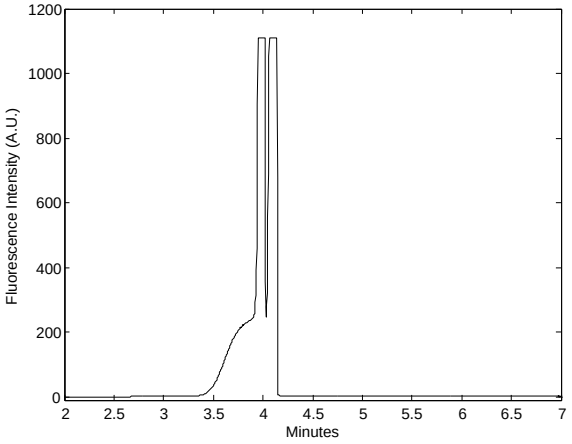

Figure 3.7 Capillary-ITP result for a 0.12 µL sample containing glutamate-FITC and phenylalanine-FITC both 50 µmol/L. The measurement using LIF shows from left to right, Phe-FITC and Glu-FITC, shown to be concentrated so far as to saturate the detector (>250 µmol/L).

The developed protocol for capillary ITP was as follows. ITP electrolytes were introduced into the fused silica capillary (27.22 cm total length, 20.38 cm from inlet to detector, 50 µm ID; Inacom Instruments, Overberg, The Netherlands) by pressure. The capillary was first flushed with trailing electrolyte (TE), 5 mmol/L of HEPES. A plug of sample was then injected, consisted of 80:20:10 TE:pretreated yeast extract:labeled amino acid solutions (v:v:v, final concentration of each amino acid 50 µmol/L) by applied pressure of 0.5 psi for 60 s which according to the Hagen-Poiseulle equation corresponds to a volume of 0.12 µL or 20% of the total capillary (6 cm). Lastly that end of the capillary was placed in a vial with leading electrolyte (LE), 10 mmol/L of NaCl, the other in one with TE. ITP was then induced by applying 5 kV. The electrolytes were prepared anew in deionized water each day, adjusted to pH 9.50 with sodium hydroxide, and stored under argon until used. Vials for experiments were covered with caps containing septa. Although sample ions migrated opposite to the EOF, at pH 9.50 the EOF was dominant. For ITP this is an advantage as more time is available to equilibrate before the analytes pass the detector.

A typical capillary ITP result is shown in Figure 3.6. Equilibrium formation could be concluded from the current during the run[129]. Spacing is seen between the bands of Glu-FITC and Phe-FITC. ITP of just the labeled amino acids only, does not show spacing (Appendix Figure 3.7). ITP of yeast alone shows negligible native fluorescence (Appendix Figure 3.11). From ITP results of each of the amino acids alone (Appendix Figures 3.12 & 3.13), showing single zones, and in the presence of yeast extract (Appendix Figures 3.14 & 3.15) showing added bands for Phe-FITC, it may be concluded that the fluorescence observed in the spacing is from Phe-FITC that interacted with compounds in the yeast biomatrix.

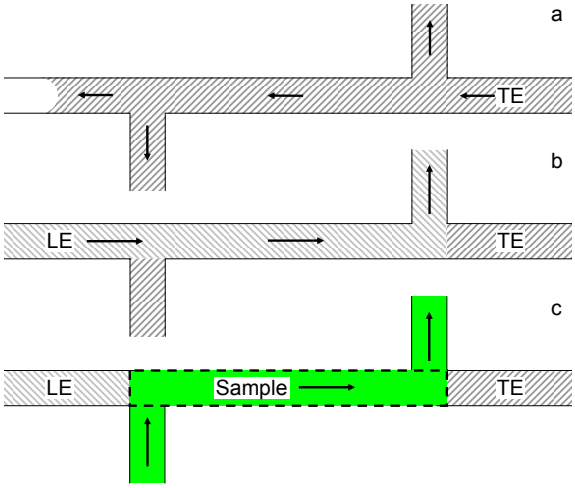

Figure 3.8 On-chip double-T injection for quantitative ITP. a) The chip is filled with trailing electrolyte by capillary filling. b) After placement of the other electrolytes in the wells, leading electrolyte is flushed towards well E, which serves as waste reservoir. c) The sample volume in the nanochannel chip (dashed box), is created by means of an exclusive EOF, from sample well D to waste E. Appropriate empirical voltage settings correspond to contanement of the fluorescence between the side channels. Settings were found to vary per channel depth. After an ITP experiment, the injection plug can be recreated by directly re-applying the sample injection voltages, e.g. those given in Figures 3.2 & 3.3.

3.7.5 Chip injection protocol

Effectively translating quantitative ITP to the nano-chip format requires a well defined sample injection volume, to be interposed between a leading electrolyte (LE) and a trailing electrolyte (TE). Here, on chip T-junctions were used in combination with EOF, see Figure 3.1. The appropriate voltage settings on the reservoirs for sample plug formation and those for ITP, were obtained empirically by observing the effects of manual voltage changes with the fluorescence microscope, see Appendix Figure 3.8 for details. The voltage settings used for the submicron channels are tabulated in Table 3.3 and those for the nanochannels in Table 3.3. These were incorporated in an automated protocol of the Labsmith Sequence software to execute the fast and/or simultaneous stepwise voltage changes required.

Table 3.3 ITP voltage steps used for 3 µm wide, 330 nm deep channels.

Well	Sample plug Figure 3.2a	Pre ITP 100 ms	ITP, Appendix Figure 3.10	ITP final Figure 3.2b
A LE	125 V	125 V	100 V	400 V
D Sample	100 V	0 V	float	float
E TE, waste	0 V	0 V	float	float
F TE	100 V	100 V	-100 V	-100 V

Table 3.4 ITP voltage steps used for 10 µm wide, 50 nm deep channels.

Well	Sample plug Figure 3.3a	ITP Figure 3.3b
A LE	25 V	100 V
D Sample	25 V	float
E TE, waste	-50 V	float
F TE	25 V	-100 V

For a nano-ITP experiment first the sample plug creation step was activated. Typically after a few minutes the plug would reform and traces of fluorescence in the separation channel were removed, allowing repeated experiments. When the stable plug was observed the ITP step was initiated manually. ITP itself was automatically preceded by a pre-ITP step of 100 ms. The pre-ITP step was needed to actively regulate the electrode in well D to zero, when set to float directly the Voltage would decrease to 0 V on a time scale of a few seconds, affecting injection accuracy. Afterwards the Voltage on well A could be increased manually to increase separation, as was done in the results in Figure 3.2b.

Implementation of the voltage settings was non-trivial and only feasible with fast and accurate computer control of the applied voltages. Switching without losing or extracting sample into or from the sidechannels proved the most critical step, being the main source of injection errors.

3.8 Appendix, Results

3.8.1 Large sample volume injections in sub-micron channels

ITP experiments were also performed on larger sample volumes, e.g. 3.2 pL (Appendix Figure 3.9). The ITP result for this larger volume demonstrated increased peak height and spacing, compared to results with smaller sample volumes (Figure 3.2). This indicates that the ITP results in Figure 3.2b & 3.3b correspond to so-called peak mode ITP[58], in contrast to plateau-mode in which case more analyte leads only to broadening of the zones[53,55]. Therefore, if more absolute amount of compound would be injected, even higher equilibrium concentrations can be expected. However, this requires either higher initial concentrations ($>$50 µmol/L) or injecting even larger volumes.

3.8.2 ITP in submicron channels at 200 V

Figure 3.10 shows the result of ITP in a 330 nm deep channel for an applied Voltage of 200 V. This result is with the injection shown in Figure 3.2a, demonstrating that 200 V is sufficient for isotachophoretic focussing but is insufficient to separate

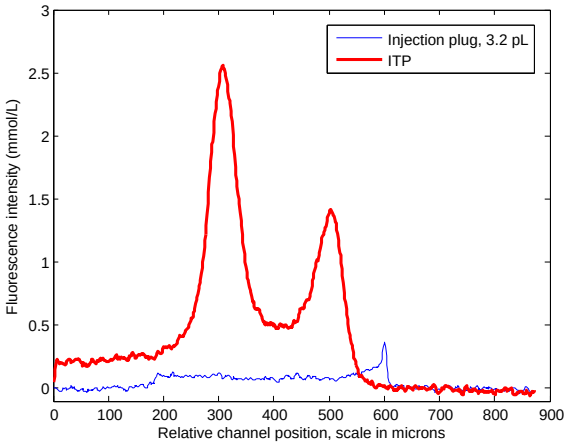

Figure 3.9 ITP result in a 330 nm deep channel. Based on the areas under the curves, the ITP result corresponds to an injection of 3.2 pL. This larger injection volume resulted in higher peaks and more spacing compared to the 0.4 pL sample in Figure 3.2c.

the amino acids. By subsequently increasing the voltage during the experiment to 500 V the separation result shown in Figure 3.2b was achieved.

3.8.3 Movie of nano ITP in a 50 nm deep channel

NanoITP.avi, in false color, background corrected and filtered. Provided in the Electronic Supporting Information of the paper this chapter was adapted from [130]

3.8.4 Additional capillary ITP Figures

Additional Figures as referenced to in section 6.4.

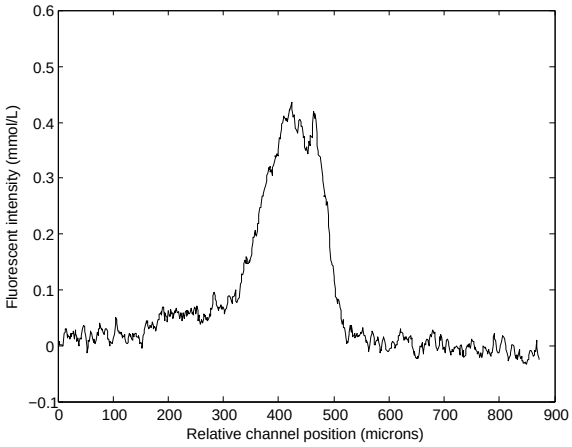

Figure 3.10 ITP foccussing result in a 330 nm deep channel, part of the same experiment as in Figure 3.2. The applied voltage difference of 200V (A = 100 V, F = -100 V).

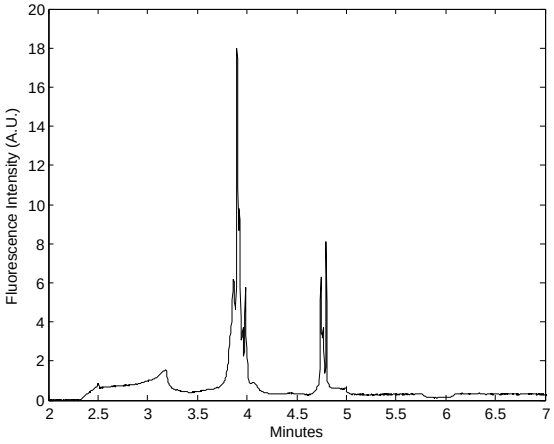

Figure 3.11 Graph showing the capillary-ITP result of yeast extract, same protocol as used for Figure 3.6.

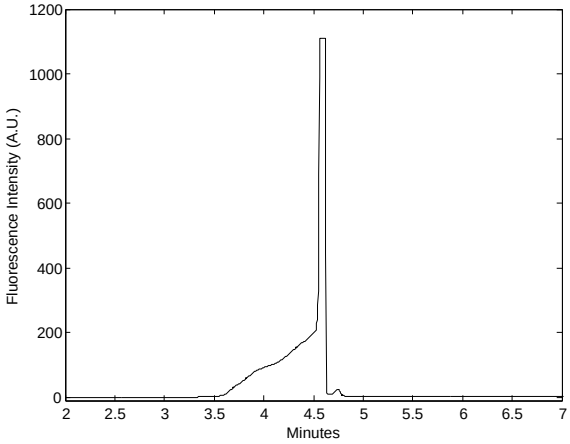

Figure 3.12 Graph showing the capillary-ITP result with 50 µmol/L phenylalanine-FITC same protocol as used for Figure 3.6.

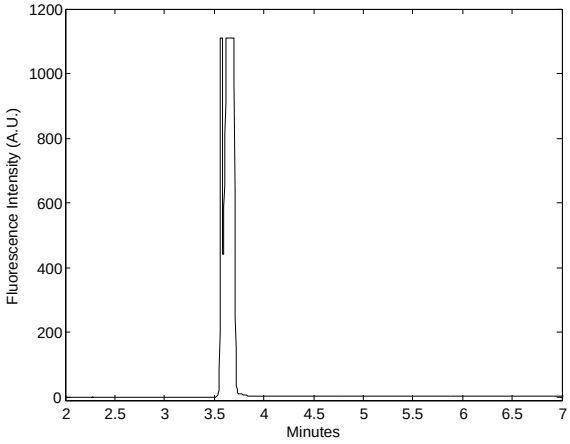

Figure 3.13 Graph showing the capillary-ITP result with 50 µmol/L glutamate-FITC same protocol as used for Figure 3.6.

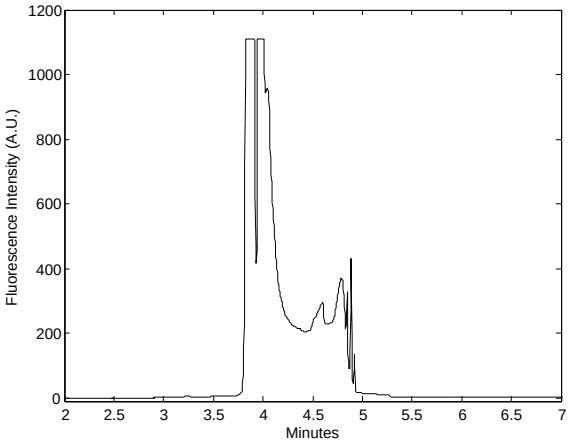

Figure 3.14 Graph showing the capillary-ITP result with 50 µmol/L phenylalanine-FITC in presence of yeast extract, same protocol as used for Figure 3.6. Clearly showing the interaction of phenylalanine-FITC with the biomatrix.

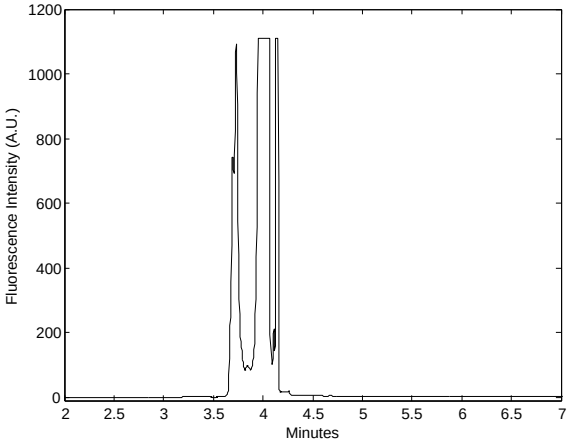

Figure 3.15 Graph showing the capillary-ITP result with 50 µmol/L glutamate-FITC in presence of yeast extract, same protocol as used for Figure 3.6.